Published in final edited form as:
J Phys Chem Lett. 2011 August 25; 2(18): 2357–2361. doi:10.1021/jz201024m.

Utilizing Lifetimes to Suppress Random Coil Features in 2D IR Spectra of Peptides

Chris T. Middleton, **Lauren E. Buchanan**, **Emily B. Dunkelberger**, and **Martin T. Zanni**
Department of Chemistry, University of Wisconsin-Madison, Madison, WI 53706-1322

Chris T. Middleton: ctmiddle@chem.wisc.edu; Lauren E. Buchanan: lbuchanan@chem.wisc.edu; Emily B. Dunkelberger: eblanco@chem.wisc.edu; Martin T. Zanni: zanni@chem.wisc.edu

Abstract

We report that the waiting time delay in 2D IR pulse sequences can be used to suppress signals from structurally disordered regions of amyloid fibrils. At a waiting time delay of 1.0 ps, the random coil vibrational modes of amylin fibrils are no longer detectable, leaving only the sharp excitonic vibrational features of the fibril β-sheets. Isotope labeling with $^{13}C^{18}O$ reveals that structurally disordered residues decay faster than residues protected from solvent. Since structural disorder is usually accompanied by hydration, we conclude that the shorter lifetimes of random-coil residues is due to solvent exposure. These results indicate that 2D IR pulse sequences can utilize the waiting time to better resolve solvent-protected regions of peptides and that local mode lifetimes should be included in simulations of 2D IR spectra.

Keywords

Protein and peptide structure; 2D IR spectroscopy; secondary structure; vibrational lifetimes; amide-I vibration; isotope labeling; amyloid fibrils; amylin

Non-linear spectroscopies, like 2D IR spectroscopy, interrogate samples using sequences of femtosecond pulses.[1,2] During the time delays between pulses, the macroscopic polarization in the sample evolves as either a coherence or population. In a coherence, the system oscillates at a vibrational frequency (or difference frequency) and decays with the homogeneous dephasing time (T_2). In a population, the system does not oscillate and decays with the vibrational lifetime (T_1). Coherence oscillations are most commonly used to study peptide and protein structures. It is a coherence that is measured in a linear infrared spectrum. The two axes of 2D IR spectra are generated by Fourier transforming the signal as a function of two different coherence delays. In principle, population times can also discriminate between signals and have been used to probe molecular structure,[3–5] but in practice there are few reports where vibrational population lifetimes in proteins and peptides differ enough to be used as structural markers.[6–8]

The peptide that we have studied is amylin, which has 37 amino acids (Fig. 1A) and assembles into long fibrils composed of columns of stacked peptides. Each column consists of two parallel β-sheets separated by a loop.[9] We prepared fibrils with $^{13}C^{18}O$ isotope

Correspondence to: Martin T. Zanni, zanni@chem.wisc.edu.

Supporting Information Available
Full methods. Version of Fig. 1A with contours plotted on a linear scale. Version of Fig. 1C with axes set to highlight BB region. Diagonal slices through spectra in Fig. 2. Description of contours used in Fig. 3. 2D IR spectra of human amylin fibrils $^{13}C^{18}O$-labeled at residues Ala8, Ala13, Ser19 and Ala25 at a waiting time of 0.5 ps. This information is available free of charge via the Internet at http://pubs.acs.org/.

labeled amylin polypeptides and measured 2D IR spectra with waiting times (Fig. 1D) of 0.0, 0.5, and 1.0 ps.

We begin by focusing on the unlabeled portion of the spectrum, which appears at frequencies >1600 cm^{-1} and is similar for all of the samples. The spectrum at 0.0 ps has the same features as previously reported for the 2D IR spectra of amylin[10–12] and is representative of Aβ,[13,14] which is another amyloid forming polypeptide. To aid in the discussion, we divide this portion of the spectra into three spectral regions, according to the historic assignments based on symmetry. These regions are the anti-symmetric β-sheet stretch (box AA), random coil (box BB), and the loop and/or symmetric β-sheet stretch (box CC). The boundaries are somewhat arbitrary, since none of the features are well resolved from one another in the spectrum at 0.0 ps. Moreover, the amide-I spectra of polypeptides are much more complicated than their empirical assignments because there are as many eigenstates as amino acids. For example, β-sheets have eigenstates that span the entire frequency range between the symmetric and antisymmetric modes,[15,16] and thus contribute throughout all 3 regions, including the random coil region BB. Besides the diagonal peaks, there are also three main sets of crosspeaks: a β-sheet/random-coil crosspeak (box AB) and two β-sheet/loop crosspeaks (box AC). All of these features decrease in intensity as a function of waiting time, but the random coil diagonal region (BB) changes both in intensity and shape.

Specifically, we observe changes in the diagonal width, the peak-to-peak separation between the fundamental and overtone peaks, and the nodal slope. Each spectral characteristic provides structural information. The diagonal width is a measure of structural and environmental disorder. Random coil structures have large diagonal widths, typically 30 cm^{-1} or more (FWHM), while amyloid β-sheets have ~15 cm^{-1} widths. The peak-to-peak separation is proportional to the anharmonic shift, which is inversely proportional to the number of oscillators contributing to the vibrational mode.[17,18] Random coil vibrations are largely localized and therefore have peak-to-peak separations of ~25 cm^{-1}, which is comparable to a single peptide linkage like N-methylacetamide (NMA).[6,19,20] In contrast, β-sheet vibrations involve many oscillators and have smaller anharmonic shifts. For example, the anti-symmetric β-sheet mode (box AA) has a peak-to-peak separation of 12 cm^{-1}. The peak-to-peak separation is not precisely the diagonal anharmonicity because of the linewidths,[2] but if a peak-to-peak separation is found that is less than that of NMA, then one can be quite confident that it is an excitonic state. A nodal slope parallel to the diagonal indicates large inhomogeneous broadening while a nodal slope parallel to the pump frequency axis indicates small inhomogeneous broadening. Because random coil structures have large structural disorder, random coil modes have nodal slopes that are more parallel with the diagonal than β-sheet. The nodal slopes of random coils can change with waiting time due to water dynamics, but the lineshape still remains largely inhomogeneous because the backbone structural disorder does not evolve on a picosecond timescale.

At 0.0 ps, the BB feature has a diagonal FWHM of 40–50 cm^{-1}, a peak-to-peak separation of 23 cm^{-1} and a nodal slope that is parallel to the diagonal (~1.0). All three observables are consistent with the 2D IR spectra of random coil polypeptides with structural and environmental disorder. Thus, at 0.0 ps, the BB region is dominated by the disordered regions of amylin, which include residues 2–7 that are constrained into a loop by a disulfide linkage, the frayed N- and C-terminal ends, and probably regions of the loop.

At 1.0 ps, the BB features are very different. The diagonal FWHM is 20–25 cm^{-1}, the peak-to-peak separation is 18 cm^{-1}, and the nodal slope is much more parallel to the pump axis (~2.7). All three observables are consistent with the excitonic vibrational mode of an

ordered structure. Thus, at 1.0 ps, we no longer observe features from random-coil structures. The spectrum is now dominated by excitonic vibrational modes.

The observation of an excitonic mode in the random coil region is consistent with simulations of β-sheets. Simulations predict that β-sheets should exhibit a localized set of states in the BB region.[15,16] These transitions arise from edge effects due to the finite sizes of actual β-sheets as compared to the symmetry allowed symmetric and antisymmetric stretches that are only rigorously preserved for infinitely large sheets. Because they are due to edge effects and not disorder, they are excitonic modes as well. Thus, the experiments suggest that the random coil regions of amylin have shorter lifetimes than the β-sheet regions.

To investigate this hypothesis further, we measured 2D IR spectra of four isotope labeled residues. Shown in Fig. 3 are 2D IR spectra collected at waiting times 0.0 and 1.0 ps for Ala8, Ala13, Ser19, and Ala25. At 0.5 ps (Fig. S1), the intensities (relative to 0.0 ps) of the four labels are 35%, 55%, 50%, and 57%, respectively. At 1.0 ps, we can no longer resolve Ala8, while the others are 8%, 9% and 32% of their original intensity, respectively. Ala25 also has a second isotope labeled peaks at 1581 cm^{-1}, which decays similarly to Ala13 and Ser19, with relative intensities of 41% and 17% at 0.5 and 1.0 ps, respectively. Thus, the amide-I band of these four amino acids have different vibrational lifetimes, with Ala8 the shortest and the 1574 cm^{-1} mode of Ala25 the longest.

The observation that β-sheet modes have longer lifetimes than random coil modes suggests that the lifetimes are correlated with structural disorder. To determine if this trend is consistent with the lifetimes of the isotopically labeled residues, we measured their peak-to-peak separations. As mentioned previously, the peak-to-peak separation is inversely proportional to the delocalization of an exciton mode, such as that formed by a column of labels in amylin fibrils (Fig. 1C). Structural and environmental disorder decreases the delocalization of excitons[21] and so peak-to-peak separations have a positive correlation with structural disorder, as observed for the β-sheet (AA) and random coil (BB) modes. All the residues measured have peak-to-peak separations smaller than NMA, indicating that they are excitonic modes. The residue with the longest lifetime, Ala25, also has smallest peak-to-peak separation of 13 cm^{-1}, compared with 18–19 cm^{-1} for the other three labels[22] Thus, Ala25 has the longest lifetime and is the most structurally ordered of the residues that we have measured in this study. The peak-to-peak separation of Ala8, which has the shortest lifetime, is comparable to Ala13 and Ser19. But since it resides at the beginning of the N-terminus β-sheet, it is likely to be more frayed than the others due to the disulfide linkage between residues 2 and 7 that forces a disordered structure. Therefore, the lifetimes of individual residues correlate with structural disorder.

A possible explanation for the correlation between vibrational lifetimes and structural disorder in amylin fibrils is that regions with structural disorder also have high levels of hydration. Solvent-exposed protein backbones generally have larger amounts of structural disorder.[23–27] Furthermore, hydrogen bonding to solvent molecules, particularly water, has been shown to accelerate vibrational relaxation in a number of small and large molecules.[28–31] In particular, the amide-I mode of the peptide backbone model N-methylacetamide has an average vibrational lifetime[32] of 0.5 ps in D_2O, 1.2 ps in DMSO and 2.0 ps in chloroform.[33] Similar lifetimes were observed by DeCamp, *et al*.[20] Theoretical studies of vibrational relaxation in cytochrome *c* suggest that water-exposed residues have shorter lifetimes than residues in the protein interior.[34] Thus, it appears that the degree of solvation alters the lifetimes of amide-I modes in extended polypeptides.

According to the solid-state NMR structural model for amylin fibrils,[9] Ala8, Ala13, and Ser19 are on the outer surface of the fibril and are therefore more solvent exposed than Ala25 which resides on the inner β-sheet of the fibril and has the longest lifetime. Of course, the precise level of backbone hydration will vary from site to site, which may account for the differences in lifetimes among the outer residues. Hydration may also explain why the two Ala25 labels have different lifetimes. Isotope labels with two peaks have been observed previously in Aβ,[35] a small β-turn peptide,[36] and an α-helix[37] which in all cases were attributed to differences in hydration.

Our group and others have learned that the inhomogeneous lineshape of the amide-I mode reflects the electrostatic disorder of the surrounding environment, which is usually dictated by the level of hydration.[20,23–25,35,38–40] The results here suggest that the vibrational lifetimes of the amide-I mode are also influence by hydration. In fact, there is a correlation between hydration (as measured by diagonal linewidths) and lifetime in previously published data on the M2 proton channel, which consists of four transmembrane α-helices that form a water filled pore (see Ref. 39, specifically Table S1 in the Supporting Information, pH 7 data of diagonal widths vs population relaxation constants). However, the correlation between vibrational lifetimes, hydration and structural disorder needs to be investigated in more systems before a reliable and intuitive correlation can be obtained. Other possible influences on the waiting time dynamics should also be explored, such as differences in relaxation rates between amide I modes or to other peptide vibrational modes[41], especially since isotope labeling alters the β-sheet vibrational modes themselves.[11,42] Nonetheless, the ability to eliminate the broad absorptions from random coil regions that congest 2D IR spectra will be very useful. It also raises the intriguing possibility that one can distinguish α-helices from random coils, which would be especially useful because they usually overlap in 1D and 2D IR spectra. We expect 2D IR waiting time dependent studies to become a highly useful method for probing protein secondary structures and hydration. We believe that 2D IR simulations should include differences in local mode lifetimes in order to properly weight contributions of secondary structure to the spectra.

Experimental Section

2D IR spectra were measured and processed using methods previously described.[12] Briefly, mid-IR pulses (60 fs, FHWM) were generated using a Ti:sapphire femtosecond laser system combined with an optical parametric amplifier and difference frequency mixing. Mid-IR pulses were split into pump and probe paths and then spatially and temporally overlapped in the sample. A mid-IR pulse shaper[43,44] was used to generate pump pulse pairs with a computer-controlled time delay that was scanned on a shot-by-shot basis. The delay between pump pulses was scanned from 0 to 2544 fs in 24 fs steps. The waiting time delay was set with a optical delay line with motorized translation state. After the sample, the probe beam was frequency resolved with a spectrometer, and detected on a shot-by-shot basis with a 64-element linear MCT array. The spectral resolution along the probe frequency axis was ~8 cm^{-1}. The polarization of the pump pulses were set perpendicular to the probe pulse.

Peptides was synthesized and purified as previous described.[45,46] Labeled amino acids labeled were also prepared as previously reported.[47,48] Purified peptides were dissolved to 1 mM concentration stock solutions in deuterated hexafluoroisopropanol. A portion of the stock solution was aliquoted dried under nitrogen and then reconstituted in 5 μL of 20 mM phosphate D_2O buffer solution (pD 7.4) to initiate aggregation. Sample were immediately transferred to a IR sample cell with CaF_2 windows and a 56 μm Teflon spacer. Samples were kept under dry air to prevent hydrogen exchange with ambient water vapor.

Supplementary Material

Refer to Web version on PubMed Central for supplementary material.

Acknowledgments

Support for this research was provided by the NIH grants DK79895 and the NSF through a CRC grant CHE 0832584. We thank Dr. Robert Tycko for providing coordinates for the structural model of amylin fibrils.

References

1. Mukamel, S. Principles of Nonlinear Optical Spectroscopy. Oxford Univ. Press; 1994.
2. Hamm, PH.; Zanni, M. Concepts and Methods of 2D Infrared Spectroscopy. Cambridge University Press; Cambridge, UK: 2011.
3. Rubtsov IV, Wang J, Hochstrasser RM. Dual-Frequency 2D-IR Spectroscopy Heterodyned Photon Echo of the Peptide Bond. P Natl Acad Sci USA. 2003; 100:5601–5606.
4. Khurmi C, Berg MA. Parallels between Multiple Population-Period Transient Spectroscopy and Multidimensional Coherence Spectroscopies. J Chem Phys. 2008; 129:064504–17. [PubMed: 18715082]
5. Rubtsov IV. Relaxation-Assisted Two-Dimensional Infrared (RA 2DIR) Method: Accessing Distances over 10 Å and Measuring Bond Connectivity Patterns. Acc Chem Res. 2009; 42:1385–1394. [PubMed: 19462972]
6. Hamm P, Lim M, Hochstrasser RM. Structure of the Amide I Band of Peptides Measured by Femtosecond Nonlinear-Infrared Spectroscopy. J Phys Chem B. 1998; 102:6123–6138.
7. Hamm P, Lim M, DeGrado WF, Hochstrasser RM. Pump/Probe Self Heterodyned 2D Spectroscopy of Vibrational Transitions of a Small Globular Peptide. J Chem Phys. 2000; 112:1907–1916.
8. Woutersen S, Mu Y, Stock G, Hamm P. Subpicosecond Conformational Dynamics of Small Peptides Probed by Two-Dimensional Vibrational Spectroscopy. P Natl Acad Sci USA. 2001; 98:11254–11258.
9. Luca S, Yau WM, Leapman R, Tycko R. Peptide Conformation and Supramolecular Organization in Amylin Fibrils: Constraints from Solid-State NMR. Biochemistry. 2007; 46:13505–13522. [PubMed: 17979302]
10. Shim SH, Gupta R, Ling YL, Strasfeld DB, Raleigh DP, Zanni MT. Two-Dimensional IR Spectroscopy and Isotope Labeling Defines the Pathway of Amyloid Formation with Residue-Specific Resolution. P Natl Acad Sci USA. 2009; 106:6614–6619.
11. Strasfeld DB, Ling YL, Gupta R, Raleigh DP, Zanni MT. Strategies for Extracting Structural Information from 2D IR Spectroscopy of Amyloid: Application to Islet Amyloid Polypeptide. J Phys Chem B. 2009; 113:15679–15691. [PubMed: 19883093]
12. Middleton CT, Woys AM, Mukherjee SS, Zanni MT. Residue-Specific Structural Kinetics of Proteins through the Union of Isotope Labeling, mid-IR Pulse Shaping, and Coherent 2D IR Spectroscopy. Methods. 2010; 52:12–22. [PubMed: 20472067]
13. Kim YS, Liu L, Axelsen PH, Hochstrasser RM. Two-Dimensional Infrared Spectra of Isotopically Diluted Amyloid Fibrils from Aβ,40. P Natl Acad Sci USA. 2008; 105:7720–7725.
14. Kim YS, Hochstrasser RM. Applications of 2D IR Spectroscopy to Peptides, Proteins, and Hydrogen-Bond Dynamics. J Phys Chem B. 2009; 113:8231–8251. [PubMed: 19351162]
15. Cheatum CM, Tokmakoff A, Knoester J. Signatures of β,-Sheet Secondary Structures in Linear and Two-Dimensional Infrared Spectroscopy. J Chem Phys. 2004; 120:8201–8215. [PubMed: 15267740]
16. Lee C, Cho M. Local Amide I Mode Frequencies and Coupling Constants in Multiple-Stranded Antiparallel β,-Sheet Polypeptides. J Phys Chem B. 2004; 108:20397–20407.
17. Wang J, Hochstrasser RM. Characteristics of the Two-Dimensional Infrared Spectroscopy of Helices from Approximate Simulations and Analytic Models. Chem Phys. 2004; 297:195–219.

18. Londergan CH, Wang J, Axelsen PH, Hochstrasser RM. Two-Dimensional Infrared Spectroscopy Displays Signatures of Structural Ordering in Peptide Aggregates. Biophysical Journal. 2006; 90:4672–4685. [PubMed: 16565049]
19. Zanni MT, Asplund MC, Hochstrasser RM. Two-Dimensional Heterodyned and Stimulated Infrared Photon Echoes of N-Methylacetamide-D. J Chem Phys. 2001; 114:4579–4590.
20. DeCamp MF, DeFlores L, McCracken JM, Tokmakoff A, Kwac K, Cho M. Amide I Vibrational Dynamics of N-Methylacetamide in Polar Solvents: The Role of Electrostatic Interactions. J Phys Chem B. 2005; 109:11016–11026. [PubMed: 16852342]
21. Anderson PW. Absence of Diffusion in Certain Random Lattices. Phys Rev. 1958; 109:1492.
22. The peak-to-peak separation of Ala25 is smaller than previously reported due to higher isotope labeling efficiency
23. Mukherjee P, Krummel AT, Fulmer EC, Kass I, Arkin IT, Zanni MT. Site-Specific Vibrational Dynamics of the CD3ζ, Membrane Peptide Using Heterodyned Two-Dimensional Infrared Photon Echo Spectroscopy. J Chem Phys. 2004; 120:10215–10224. [PubMed: 15268045]
24. Mukherjee P, Kass I, Arkin IT, Zanni MT. Structural Disorder of the CD3ζ, Transmembrane Domain Studied with 2D IR Spectroscopy and Molecular Dynamics Simulations. J Phys Chem B. 2006; 110:24740–24749. [PubMed: 17134238]
25. Mukherjee P, Kass I, Arkin I, Zanni MT. Picosecond Dynamics of a Membrane Protein Revealed by 2D IR. P Natl Acad Sci USA. 2006; 103:3528–3533.
26. Wood K, Plazanet M, Gabel F, Kessler B, Oesterhelt D, Tobias DJ, Zaccai G, Weik M. Coupling of Protein and Hydration-Water Dynamics in Biological Membranes. P Natl Acad Sci USA. 2007; 104:18049–18054.
27. Wood K, Frölich A, Paciaroni A, Moulin M, Härtlein M, Zaccai G, Tobias DJ, Weik M. Coincidence of Dynamical Transitions in a Soluble Protein and Its Hydration Water: Direct Measurements by Neutron Scattering and MD Simulations. J Am Chem Soc. 2008; 130:4586–4587. [PubMed: 18338890]
28. Terazima M. Vibrational Relaxation from Electronically Photoexcited States in Solution Studied by the Acoustic Peak Delay Method: Hydrogen Bonding Effect to Betaine-30. Chem Phys Lett. 1999; 305:189–196.
29. Kovalenko SA, Schanz R, Hennig H, Ernsting NP. Cooling Dynamics of an Optically Excited Molecular Probe in Solution from Femtosecond Broadband Transient Absorption Spectroscopy. J Chem Phys. 2001; 115:3256–3273.
30. Ohta K, Tominaga K. Vibrational Population Relaxation of Thiocyanate Ion in Polar Solvents Studied by Ultrafast Infrared Spectroscopy. Chem Phys Lett. 2006; 429:136–140.
31. Middleton CT, Cohen B, Kohler B. Solvent and Solvent Isotope Effects on the Vibrational Cooling Dynamics of a DNA Base Derivative. J Phys Chem A. 2007; 111:10460–10467. [PubMed: 17910423]
32. Calculated as $f*T_S + (1-f)*T_l$ from Table 1 of Ref. 33
33. Wang L, Middleton CT, Zanni MT, Skinner JL. Development and Validation of Transferable Amide I Vibrational Frequency Maps for Peptides. J Phys Chem B. 2011; 115:3713–3724. [PubMed: 21405034]
34. Fujisaki H, Straub JE. Vibrational Energy Relaxation of Isotopically Labeled Amide I Modes in Cytochrome C: Theoretical Investigation of Vibrational Energy Relaxation Rates and Pathways. J Phys Chem B. 2007; 111:12017–12023. [PubMed: 17887785]
35. Kim YS, Liu L, Axelsen PH, Hochstrasser RM. 2D IR Provides Evidence for Mobile Water Molecules in β,-Amyloid Fibrils. P Natl Acad Sci USA. 2009; 106:17751–17756.
36. Smith AW, Lessing J, Ganim Z, Peng CS, Tokmakoff A, Roy S, Jansen TLC, Knoester J. Melting of a β,-Hairpin Peptide Using Isotope-Edited 2D IR Spectroscopy and Simulations. J Phys Chem B. 2010; 114:10913–10924. [PubMed: 20690697]
37. Backus EHG, Bloem R, Donaldson PM, Ihalainen JA, Pfister R, Paoli B, Caflisch A, Hamm P. 2D-IR Study of a Photoswitchable Isotope-Labeled α,-Helix. J Phys Chem B. 2010; 114:3735–3740. [PubMed: 20166694]
38. Fang C, Hochstrasser RM. Two-Dimensional Infrared Spectra of the $^{13}C{=}^{18}O$ Isotopomers of Alanine Residues in an α,-Helix. J Phys Chem B. 2005; 109:18652–18663. [PubMed: 16853400]

39. Manor J, Mukherjee P, Lin YS, Leonov H, Skinner JL, Zanni MT, Arkin IT. Gating Mechanism of the Influenza a M2 Channel Revealed by 1D and 2D IR Spectroscopies. Structure. 2009; 17:247–254. [PubMed: 19217395]
40. Woys AM, Lin YS, Reddy AS, Xiong W, de Pablo JJ, Skinner JL, Zanni MT. 2D IR Line Shapes Probe Ovispirin Peptide Conformation and Depth in Lipid Bilayers. J Am Chem Soc. 2010; 132:2832–2838. [PubMed: 20136132]
41. Kurochkin DV, Naraharisetty SRG, Rubtsov IV. A Relaxation-Assisted 2D IR Spectroscopy Method. P Natl Acad Sci USA. 2007; 104:14209–14214.
42. Wang J, Chen J, Hochstrasser RM. Local Structure of β,-Hairpin Isotopomers by Ftir, 2D IR, and Ab Initio Theory. J Phys Chem B. 2006; 110:7545–7555. [PubMed: 16599536]
43. Shim SH, Strasfeld DB, Zanni MT. Generation and Characterization of Phase and Amplitude Shaped Femtosecond mid-IR Pulses. Opt Express. 2006; 14:13120–13130. [PubMed: 19532209]
44. Shim SH, Strasfeld DB, Fulmer EC, Zanni MT. Femtosecond Pulse Shaping Directly in the mid-IR Using Acousto-Optic Modulation. Opt Lett. 2006; 31:838–840. [PubMed: 16544641]
45. Marek P, Woys AM, Sutton K, Zanni MT, Raleigh DP. Efficient Microwave-Assisted Synthesis of Human Islet Amyloid Polypeptide Designed to Facilitate the Specific Incorporation of Labeled Amino Acids. Org Lett. 2010; 12:4848–4851. [PubMed: 20931985]
46. Abedini A, Raleigh DP. Incorporation of Pseudoproline Derivatives Allows the Facile Synthesis of Human IAPP, a Sighly Amyloidogenic and Aggregation-Prone Polypeptide. Org Lett. 2005; 7:693–696. [PubMed: 15704927]
47. Marecek J, Song B, Brewer S, Belyea J, Dyer RB, Raleigh DP. A Simple and Economical Method for the Production of ^{13}C,^{18}O-Labeled Fmoc-Amino Acids with High Levels of Enrichment: Applications to Isotope-Edited IR Studies of Proteins. Org Lett. 2007; 9:4935–4937. [PubMed: 17958432]
48. Seyfried MS, Lauber BS, Luedtke NW. Multiple-Turnover Isotopic Labeling of Fmoc- and Boc-Protected Amino Acids with Oxygen Isotopes. Org Lett. 2009; 12:104–106. [PubMed: 20035564]

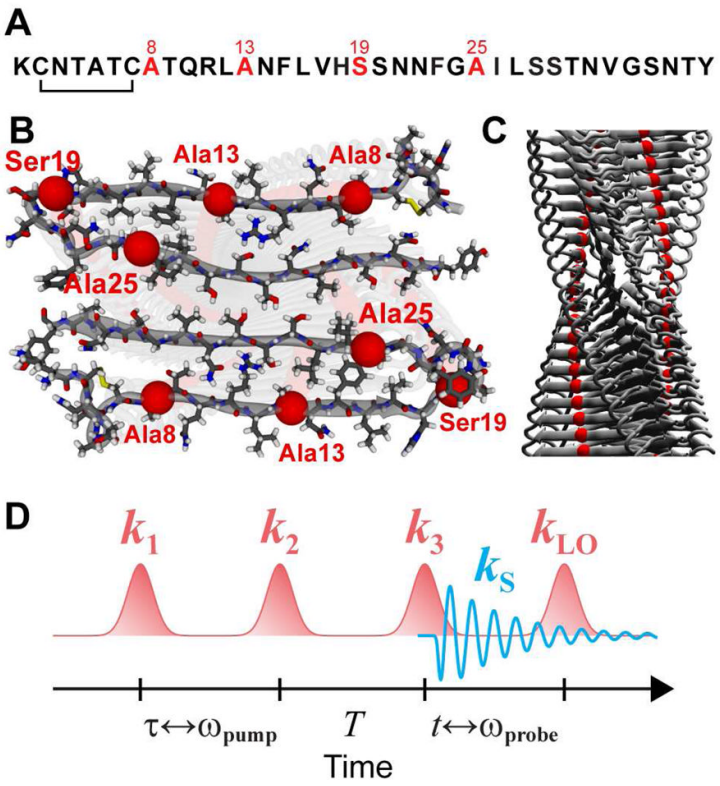

Fig. 1.

(A) Amino-acid sequence of amylin polypeptide. Residues Cys2 and Cys7 are joined by a disulphide bond. Residues which were $^{13}C^{18}O$ labels were used are red. (B) Depiction of a single amylin fibril layer (top view). Residues where $^{13}C^{18}O$ isotope labels were used are denoted with red spheres. (C) Depiction of a single amylin fibril layer (side view). Labeling of a single residue, Ala13 (red spheres) for example, creates linear chains of labels in the fibril. (D) Pulse sequence used in 2D IR experiments. The pump and probe frequency axes are generated by Fourier transform over τ and *T*, respectively. Spectra are recorded at a series of waiting times, *T*.

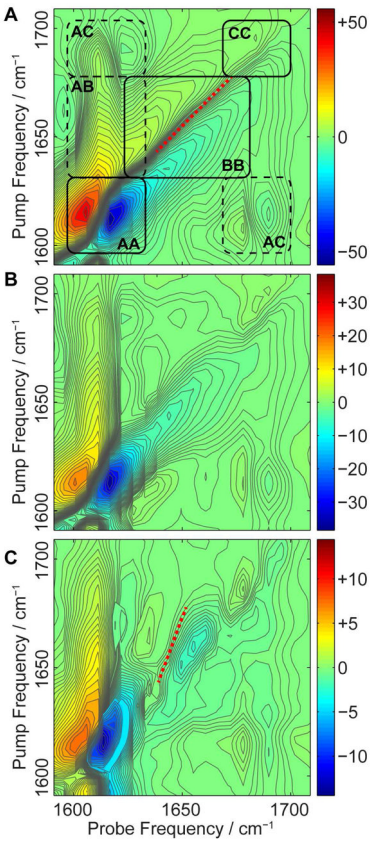

Figure 2.

2D IR spectra of human amylin fibrils with $^{13}C^{18}O$ labels at Ala13 and waiting times of (A) 0.0 ps, (B) 0.5 ps, (C) 1.0 ps. Nodal slopes measured for the BB region are drawn with red dashed lines. Spectral amplitudes are plotted on an logarithmic scale.

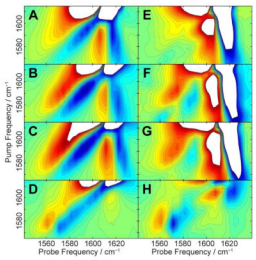

Figure 3.

2D IR spectra of $^{13}C^{18}O$-labeled human amylin fibrils at waiting times of 0.0 ps (A–D) and 1.0 ps (E–H). Spectra correspond to labels at residues Ala8 (A,E), Ala13 (B,F), Ser19 (C,G), and Ala25 (D,H). Amplitudes are plotted on a linear scale.